# Signal Output of Triboelectric Nanogenerator at Oil–Water–Solid Multiphase Interfaces and its Application for Dual-Signal Chemical Sensing

*Peng Jiang, Lei Zhang, Hengyu Guo, Chaoyu Chen, Changsheng Wu, Steven Zhang, and Zhong Lin Wang\**

A liquid–solid contact triboelectric nanogenerator (TENG) based on poly(tetrafluoroethylene) (PTFE) film, a copper electrode, and a glass substrate for harvesting energy in oil/water multiphases is reported. There are two distinctive signals being generated, one is from the contact electrification and electrostatic induction between the liquid (water/oil) and the PTFE film ($V_{TENG}$ and $I_{TENG}$); and the other is from the electrostatic induction in the copper electrode by the oil/water interfacial charges ($\Delta V_{interface}$ and $I_{interface}$), which is generated only when the liquid–solid contact TENG is inserted across the oil/water interface. The two signals show interesting opposite changing trends that the $V_{TENG}$ and $I_{TENG}$ decrease while the oil/water interfacial signals of $\Delta V_{interface}$ and $I_{interface}$ increase after coating a layer of polydopamine on the surfaces of PTFE and glass via self-polymerization. As an application of the observed phenomena, both the values of $I_{TENG}$ and $I_{interface}$ have a good linear relationship versus the natural logarithm of the concentration of the dopamine. Based on this, the first self-powered dual-signal detection of dopamine using TENG is demonstrated.

Harvesting ambient mechanical energy not only provides a viable means of producing renewable energy, but also opens up a new path to self-powered sensors/systems without an external power source. The triboelectric nanogenerator (TENG), which was first invented by the Wang group in 2012, is a kind of device that can effectively convert ambient and distributed mechanical energy, such as wind energy, body motion energy, and vibration energy, into electrical output by coupling triboelectric effect and electrostatic induction.[1] The converted electrical energy can be used not only as a power source but also as a signal for biochemical sensing, because the electrical output signals can be significantly affected by molecules adsorbed on the contact surface of TENG. To date, many different types of self-powered biochemical sensors based on TENG for the detection of catechin, dopamine, phenol, thrombin, heavy metal ions, etc. have been demonstrated.[2] However, most of these sensors relied on the solid–solid contact electrification, which have some issues such as durability and output stability due to the cross-contamination that resulted from adsorption of chemicals during the contact of triboelectric layers. Moreover, the humidity and surface roughness may also affect the output of TENG,[3] thus affects the accuracy of analysis as a biochemical sensor.

Recently, liquid–solid contact TENG has also been successfully designed for harvesting water wave energy and developed as self-powered sensors for solution temperature, polarity, and chemical concentration.[4] As a chemical sensor, the liquid–solid contact TENG has many advantages over solid–solid contact TENG. It not only overcomes the issues existing in solid–solid contact TENG as mentioned above, but also is more flexible for the development of various miniaturized chemical sensors, such as microfluidic chips sensors and capillary tube sensors.[5] However, as one of the most important kinds of TENG, the current study of liquid–solid contact TENG is only based on a single liquid phase, and there are no reports focusing on the liquid–solid contact TENG in oil/water multiphase systems. Oil/water mixtures are ubiquitous in nature and the oil/water interfacial charges are particularly important in chemistry, physics, engineering, biology, and life sciences.[6] It has long been known that the oil/water interface can acquire negative charges,[7–9] which is a potential energy source that can be harvested by TENG.

Here, a single-electrode liquid–solid contact TENG has been fabricated with poly(tetrafluoroethylene) (PTFE) film, a copper

Dr. P. Jiang, L. Zhang, H. Guo, C. Chen, C. Wu, S. Zhang,
Prof. Z. L. Wang
School of Materials Science and Engineering
Georgia Institute of Technology
Atlanta, GA 30332, USA
E-mail: zhong.wang@mse.gatech.edu
Dr. P. Jiang
School of Pharmaceutical Sciences
Wuhan University
Wuhan 430071, P. R. China
Prof. Z. L. Wang
Beijing Institute of Nanoenergy and Nanosystems
Chinese Academy of Sciences
Beijing 100083, P. R. China

The ORCID identification number(s) for the author(s) of this article can be found under https://doi.org/10.1002/adma.201902793.

**ADVANCED
SCIENCE NEWS**

www.advancedsciencenews.com
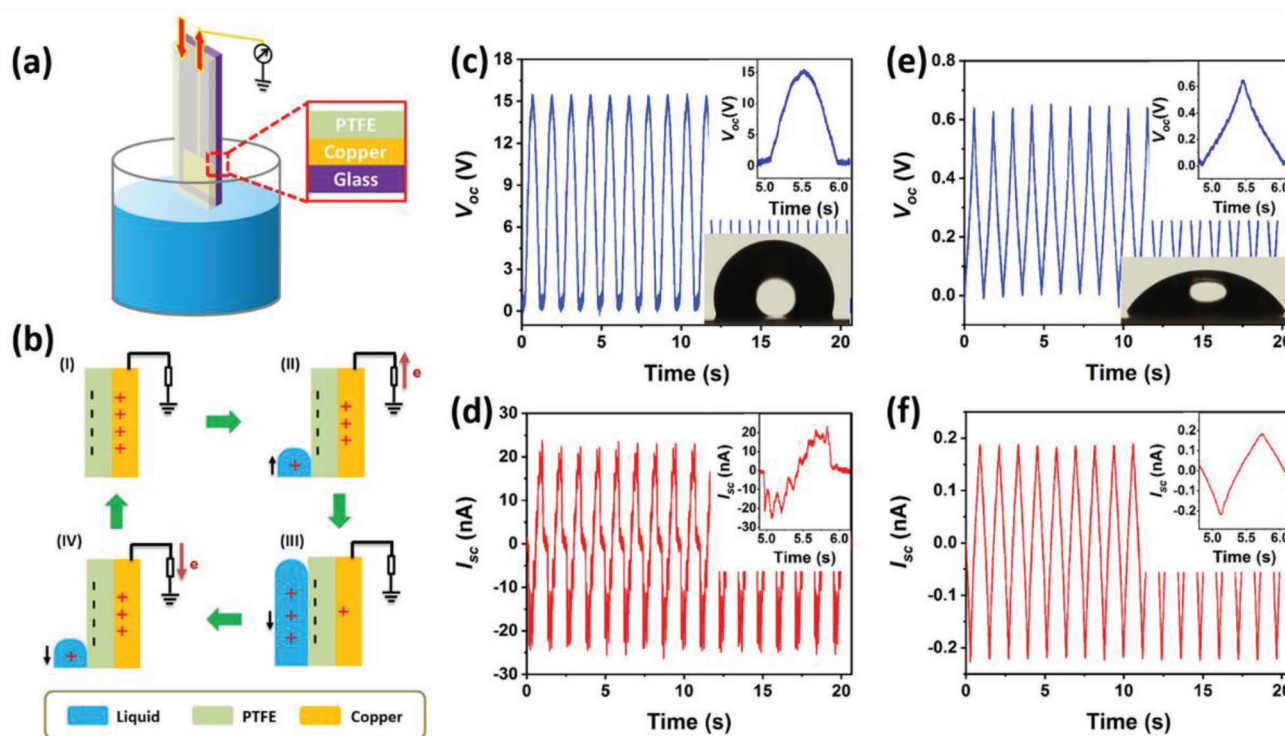
**ADVANCED
MATERIALS**

www.advmat.de

**Figure 1.** a) Schematic illustration of the liquid–solid TENG and b) its electricity-generating process. c–f) Open-circuit voltage ($V_{oc}$) and short-circuit current ($I_{sc}$) of the liquid–solid TENG in water (c,d) and paraffin oil (e,f). Insets (c–f): enlarged view of single cycle and contact angle image of water and paraffin oil on PTFE.

electrode, and a glass substrate (**Figure 1**a) to investigate the signal output of TENG at oil–water–solid multiphase interfaces. Two distinctive signals were obtained when the liquid–solid contact TENG was inserted into the oil/water multiphase, one is from the contact electrification and electrostatic induction between the liquid and the PTFE film, and the other one is from the electrostatic induction in the copper electrode by the oil/water interfacial charges. These two distinctive signals provide an excellent self-powered dual-signal platform for biochemical sensing and has been successfully demonstrated for dopamine (DA) detection. In some complex samples, such as biological matrix, a single signal detection may cause false-positive or false-negative results. In comparison, the dual-signal detection system can improve the accuracy of detection. To the best of our knowledge, this is the first self-powered dual-signal biochemical sensing platform based on TENG.

The structure of the single-electrode liquid–solid contact TENG is shown in Figure 1a. The substrate is a plain glass slide (75 mm × 25 mm × 1 mm). A 20 mm × 15 mm rectangular copper electrode was deposited on the glass slide substrate by physical vapor deposition (PVD). On the vertical direction of the electrode, a 2 mm wide strip-shaped copper was deposited for connecting the copper electrodes and external wires. An electrification thin film made of PTFE was tightly adhered to the surface of the glass slide on the copper electrode side to insulate the copper electrode from the surrounding liquid. PTFE is a good electrification material for the fabrication of liquid–solid contact TENG not only due to its strong capability to obtain electrons after contact electrification with most materials,[10] but

also due to its good hydrophobicity to avoid a decrease of electric output caused by electrostatic screening.[11] The liquid–solid contact TENG was operated by periodically inserting it into and pulling out of solution to generate electric output (Figure 1a). The electricity generation mechanism can be explained as a result of contact electrification and electrostatic induction due to the emerging and submerging TENG to liquid, which drives the electron exchange between the triboelectrode (copper electrode) and ground. Figure 1b illustrates the electricity generation process of a complete cycle. PTFE is a highly negative material in the triboelectric series, and it is reported that negative charges will be generated at the PTFE surface due to contact electrification when the PTFE contact with liquid (e.g., water), and the negative charge layer on the PTFE surface will not dissipate in an extended period of time, even though the TENG has been pulled out of water.[11,12] In this case, positive charges will be induced into the copper electrode to maintain electrostatic equilibrium, as shown in Figure 1b(I). When the TENG is gradually inserted into the water again, the negative charge layer on the PTFE surface will be partially screened by forming an electrical double layer, which will induce electrons to flow from the ground to the copper electrode to reneutralize the unbalanced charges distributed between the triboelectric layer and copper electrode (Figure 1b(II)). This process will reach an equilibrium state when the copper electrode is completely immersed in water (Figure 1b(III)). As the TENG is pulled out of the water, the positive charges in water at the PTFE–water interface will be removed from the surface of PTFE due to its good hydrophobicity, while the negative charges remain on the
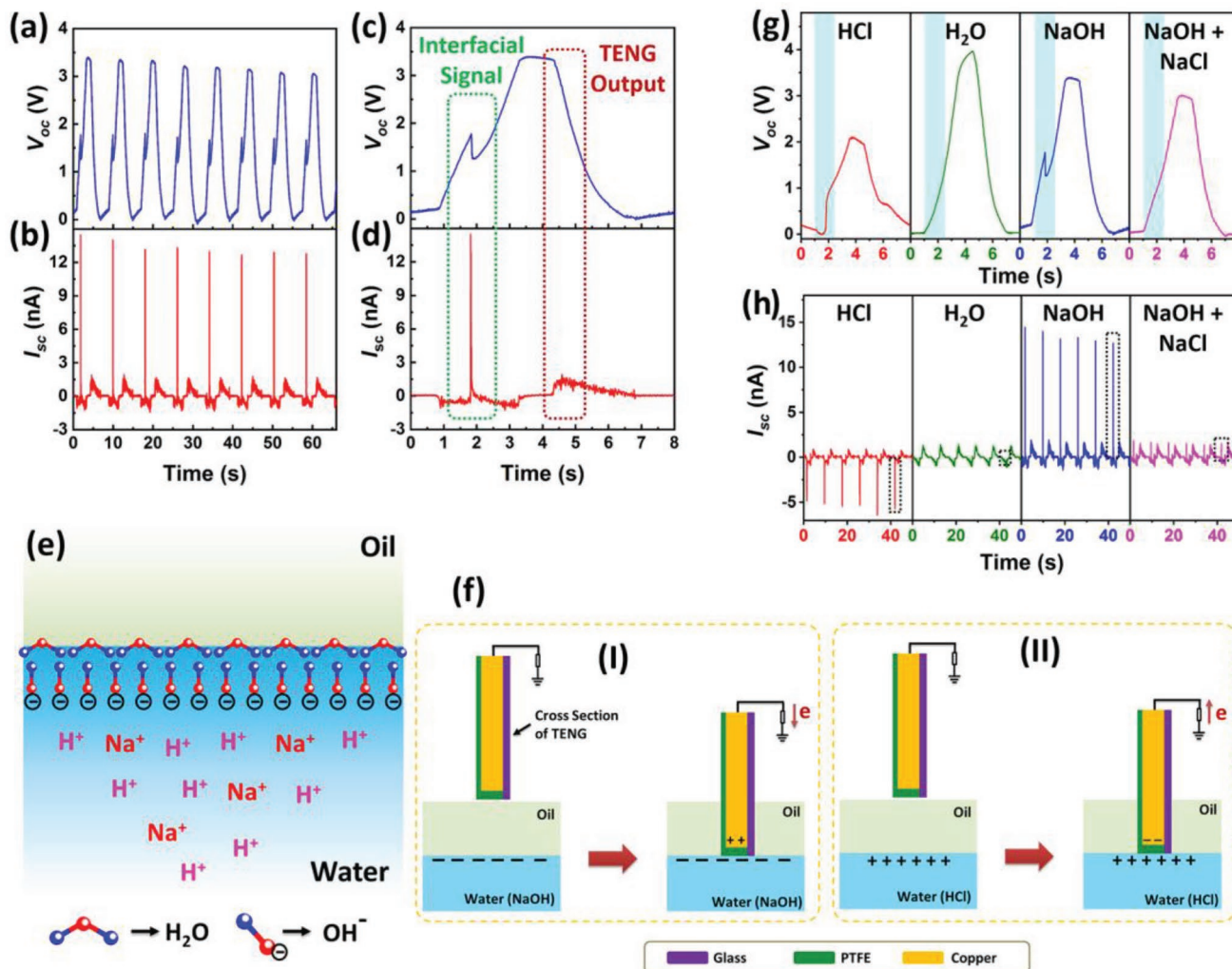
ADVANCED
SCIENCE NEWS
www.advancedsciencenews.com

ADVANCED
MATERIALS
www.advmat.de

**Figure 2.** a) Open-circuit voltage ($V_{oc}$) and b) short-circuit current ($I_{sc}$) of TENG in paraffin oil/water (NaOH, 0.1 mol L$^{-1}$) multiphase. c,d) Enlarged view of single cycle of $V_{oc}$ and $I_{sc}$. e) Schematic illustration of oil/water interfacial charges and f) the interfacial signal-generating process. g,h) $V_{oc}$ and $I_{sc}$ of TENG in paraffin oil/water with different aqueous solutions of HCl (0.1 mol L$^{-1}$), deionized water, NaOH (0.1 mol L$^{-1}$), and mixture solution of NaOH and NaCl (0.1 mol L$^{-1}$). Operation speed: 0.01 m s$^{-1}$.

PTFE surface. To maintain electrostatic equilibrium, electrons will be induced to flow from the copper electrode to the ground (Figure 1b(III)) until reaching an equilibrium state when the electrode is completely out of water (Figure 1b(IV)). We first measured the open-circuit voltage ($V_{oc}$) and short-circuit current ($I_{sc}$) of the liquid–solid contact TENG in single liquid phase of water and paraffin oil (Figure 1c–f), respectively. As demonstrated in the contact angle image in Figure 1c,e, the PTFE film is hydrophobic to water and lipophilic to oil. The $V_{oc}$ for water and paraffin oil are approximately 15 and 0.65 V, respectively, and the $I_{sc}$ are approximately 25 and 0.22 nA, respectively. The enlarged view of single cycle of $I_{sc}$ (insets in Figure 1c–f) shows that the short-circuit current has an alternating behavior during the single cycle of inserting and pulling out TENG of solution, which matches well with the electricity generation mechanism discussed above.

To investigate the performance of the TENG in oil/water multiphase, the TENG was operated by periodically inserting it into and pulling out of paraffin oil/NaOH solution multiphase and measuring the $V_{oc}$ and $I_{sc}$ (**Figure 2**a–d). It has long been known that oil drops in the absence of surfactants spontaneously acquire negative charges and migrate toward the positive electrode in an electrophoresis cell.[7] The pH dependence of the electrophoretic mobility of the oil droplet, which increased with increasing pH of the aqueous phase, suggesting that the negative interfacial charges originated from preferential adsorption of hydroxyl ions (OH$^-$) at the oil/water interface.[8,13,14] A reliable explanation of preferential OH$^-$ adsorption is that the interfacial water molecules are preferentially oriented with the oxygen atoms toward the hydrophobic phase, thus adsorbing OH$^-$ through the strong dipole or hydrogen bonding of the OH$^-$ ions with the hydrogen atoms of the interfacial water molecules (as shown in Figure 2e).[14] Therefore, when the bottom of the TENG contacts the oil/water interface, the negative charges at the interface will induce an interfacial voltage drop ($\Delta V_{interface}$) and a corresponding interfacial current ($I_{interface}$)

by electrostatic induction (Figure 2f). The single cycle of $V_{oc}$ (Figure 2c) shows that a significant voltage drop of approximately 0.5 V appears when the bottom of the electrode contacts the oil–water interface. Correspondingly, a current pulse of approximately 14.7 nA appears simultaneously in the $I_{sc}$ curve. The interfacial signals of $\Delta V_{interface}$ and $I_{interface}$ also appear at different operating speeds of 0.1, 0.05, and 0.02 m s$^{-1}$, as shown in Figure S1, Supporting Information. The electrical performance at different oil depths is also measured. As shown in Figure S2, Supporting Information, the interface current peaks at different oil depths appear at approximately 1.04, 2.02, and 3.55 s, respectively, at a moving speed of 1 cm s$^{-1}$ (taking the bottom of the electrode to contact the oil surface as the starting point), which matches well with the depth of the oil of 1.0, 2.0, and 3.5 cm. Hexadecane, another widely used oil in the study of oil/water interfacial potential, is also used as the oil phase to investigate the electrical performance of the liquid–solid TENG in oil/water multiphase (Figure S3, Supporting Information). Similar to the results of paraffin oil, the interfacial signal of $\Delta V_{interface}$ and $I_{interface}$ also appears when the TENG contacts the oil/water interface. Moreover, the liquid–solid TENG were also fabricated with other materials, such as FEP film with glass substrate, PTFE film with acrylic substrate, to investigate the oil/water interfacial signal. The results show that the interfacial signals of $\Delta V_{interface}$ and $I_{interface}$ also appear when these TENGs are operated in the paraffin oil/water (NaOH) multiphase (as shown in Figure S4, Supporting Information).

To further confirm that the interfacial signals ($\Delta V_{interface}$ and $I_{interface}$) are caused by the negative interfacial charges, the performance of the TENG in oil/water multiphase are compared by using HCl (0.1 mol L$^{-1}$), deionized water, NaOH (0.1 mol L$^{-1}$), and a mixture solution of NaOH and NaCl (0.1 mol L$^{-1}$) as the water phase separately (Figure 2g,h and Figure S5, Supporting Information). It is reported that the oil/water interfacial potential is negative, as mentioned above, and the negative oil/water interfacial potential decreases with decreasing pH of the aqueous phase and even becomes positive with strong acid aqueous phase.[15] As shown in Figure 2g,h, there are obvious interfacial signals of $\Delta V_{interface}$ and $I_{interface}$ in the oil/NaOH multiphase, which are approximately 0.5 V and 14.7 nA, respectively. In contrast, the interfacial signals are very weak in the deionized water–based oil/water multiphase. More importantly, when the water phase is changed to a strong acidic HCl solution (0.1 mol L$^{-1}$), the interfacial signals are even reversed, resulting in a voltage increase and a corresponding reverse current pulse at the oil/water interface. These results are consistent with the reported pH dependence of the oil/water interface potential, indicating that the interfacial signals measured from the TENG are derived from the oil/water interface potential.[14,15] To further support the inference, the electric potential distribution on the electrode when the TENG passes through the negative and positive oil/water interface was simulated by COMSOL (Figure S6, Supporting Information). The simulation results for both the negative and positive oil/water interface (Figure S6e,j, Supporting Information) are well matched to the open-circuit voltage curve of the NaOH and HCl solution, respectively, as shown in Figure 2g. It can be concluded that the interfacial signal is from the electrostatic induction in the copper electrode by the oil/water interfacial charges (Figure 2f).

As a controlled experiment, the performance of TENG in a single aqueous phase of HCl (0.1 mol L$^{-1}$), deionized water, and NaOH (0.1 mol L$^{-1}$) were also measured. As shown in Figure S7, Supporting Information, the interfacial signals of $\Delta V_{interface}$ and $I_{interface}$ do not appear in these single aqueous phases, and the electrical output decreases in both HCl and NaOH solution. By comparing the results of NaOH and the mixture of NaOH and NaCl solution (Figure 2g,h), it can be seen that the interfacial signals are significantly decreased after adding NaCl to the NaOH solution, which is also consistent with the reported double-layer compression effect of the oil/water interface that the interfacial potential reduces with increasing NaCl concentration.[16]

The liquid–solid TENG in oil/water multiphase can generate two different signals (Figure 2a–d), as discussed above, one is from the contact electrification and electrostatic induction between the liquid and the PTFE film (called $V_{TENG}$ and $I_{TENG}$), and the other is from the electrostatic induction of the oil/water interfacial charges (called $\Delta V_{interface}$ and $I_{interface}$). These two distinctive signals provide a good self-powered dual-signal platform for biochemical sensing. In this work, a dopamine detection method based on this dual-signal platform was developed to demonstrate its potential as a biochemical sensor. Dopamine is an important neurotransmitter for the function of the central nervous systems, and its physiological level is related to neurological diseases such as Parkinson's disease, Huntington's disease, and schizophrenia.[17] The dual-signal dopamine sensing process is shown in **Figure 3**a. Firstly, the TENG device is immersed in a dopamine solution (pH 8.5 Tris-HCl buffer) to form a polydopamine (PDA) layer on the PTFE and glass surfaces of the TENG via the self-polymerization of dopamine. The PDA layer can firmly adhere to the PTFE and glass surfaces via the strong binding affinity of catechol functional groups, as shown in the scanning electron microscopy (SEM) images in Figure 3b. The photographs of PTFE and glass after being modified by dopamine with concentration of 25–500 µmol L$^{-1}$ show that the PDA coating in PTFE and glass have good uniformity (Figure S8a,b, Supporting Information). The absorption spectra of dopamine-modified glass demonstrate that the amount of PDA absorbed on the TENG surface increases as the dopamine concentration increases (Figure S8c, Supporting Information). Then the electrical performance of the TENG without and with PDA layer were both measured in the oil/water multiphase (Figure 3c,d, Supporting Information). A pH 8.5 Tris-HCl buffer was used as the aqueous phase because the PDA layer is not stable under strong basic solution. As shown in Figure 3c,d, the electrical outputs at an operating speed of 0.01 m s$^{-1}$ show interesting opposite changing trends for the dual signals after coating a layer of PDA in a 250 µmol L$^{-1}$ dopamine solution, that is, the $V_{TENG}$ and $I_{TENG}$ decrease significantly from approximately 4.5 to 1.3 V and 1.9 to 0.4 nA, respectively, while the oil/water interfacial signal of $\Delta V_{interface}$ and $I_{interface}$ increases significantly from approximately 0.02 to 0.1 V and 0.7 to 6.5 nA, respectively. The reported radical-scavenging property of PDA,[18] which can dramatically reduce the amount of surface charge generated by contact electrification, may be the main reason for the decrease of $V_{TENG}$ and $I_{TENG}$. Moreover, the enhanced hydrophilicity after coating PDA layer, which can increase the electrostatic screening, may be another
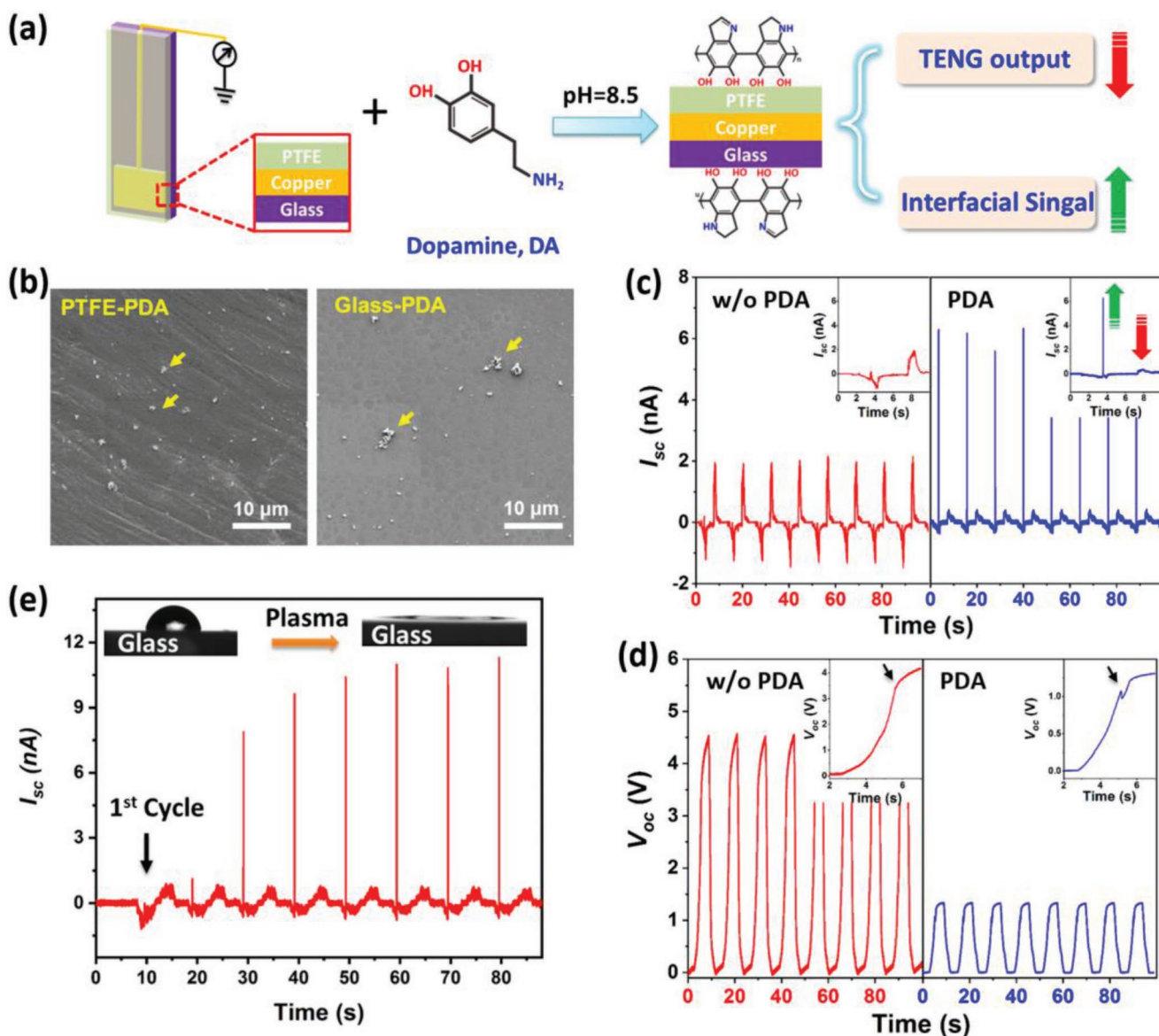
**Figure 3.** a) Schematic illustration of dopamine polymerization on the surface of TENG. b) SEM images of PTFE and glass with PDA coating. c) Short-circuit current ($I_{sc}$) and d) open-circuit voltage ($V_{oc}$) of liquid–solid TENG in oil/water (pH 8.5 Tris-HCl buffer) multiphase without (w/o) and with PDA coating. e) $I_{sc}$ of the plasma-treated TENG measured during the first few periodic insertion and pull cycles. Inset in (e): contact angle images of water on glass surface without (w/o) (left) and with (right) plasma treatment.

reason for the decrease of $V_{TENG}$ and $I_{TENG}$. On the other hand, the increased hydrophilicity can result in much more adsorption of the aqueous solution on the surface of TENG, which can increase the conductivity of the surface of the TENG and thereby enhancing the electrostatic induction between the copper electrode and interfacial charges, this may be the reason for the increase of the interface signal of $\Delta V_{interface}$ and $I_{interface}$. To further understand the effect of surface hydrophilicity on the interface signal, the glass surface of the TENG was treated with plasma (Figure S9, Supporting Information). The contact angle image (Figure 3e) shows that the glass surface becomes superhydrophilic after plasma treatment. The electrical output of the liquid–solid TENG without and with plasma treatment shows that the interfacial signal increases significantly after

plasma treatment (Figure S9b–d, Supporting Information). However, when the plasma-treated glass surface is covered by a hydrophobic PTFE film, these interfacial signal will disappear (as shown in Figure S10, Supporting Information). These results indicate that the surface hydrophilicity of the TENG glass surface is critical for generating interfacial signal in oil/water multiphase. To further support the inference that the increased interfacial signal is attributed to the aqueous solution adsorption on the TENG surface, the short-circuit current of the plasma-treated TENG during the first few periodic insertion and pull cycles was recorded. As shown in Figure 3e, in the first cycle, there is no interfacial signal because there is no water layer adsorption on the TENG surface. After the first cycle, the water layer gradually adsorbs on the TENG surface,
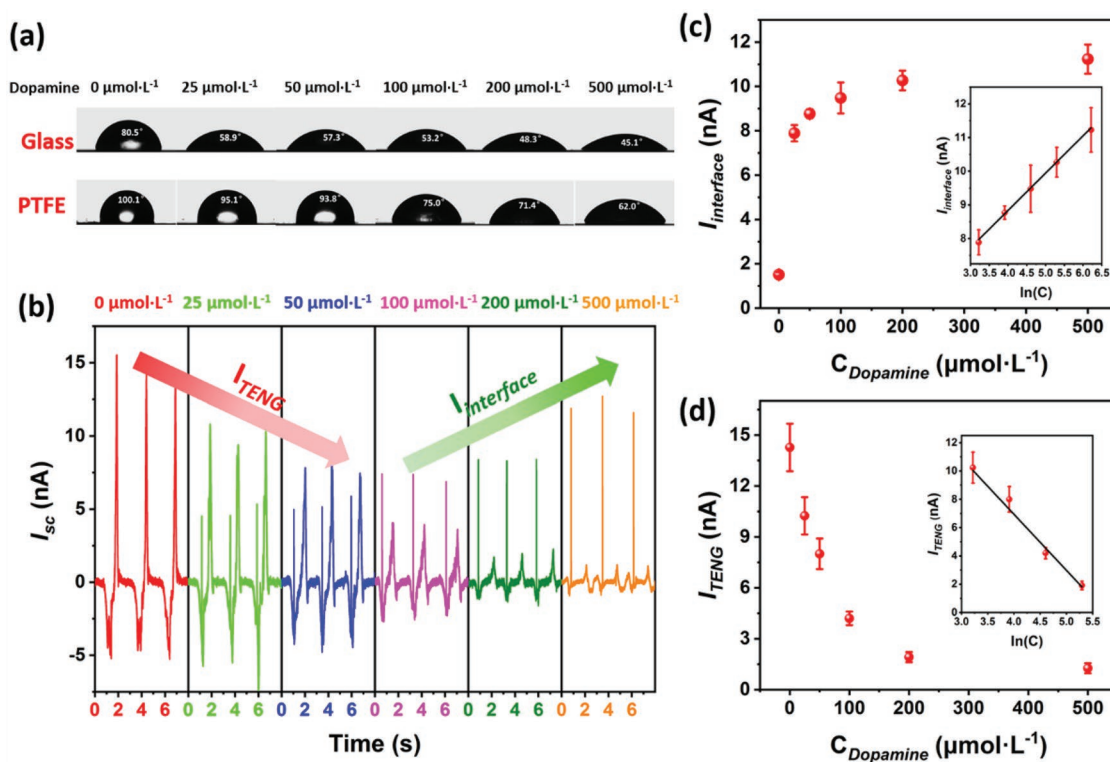
**Figure 4.** a) Contact angle images of water on glass and PTFE surface after being modified by dopamine with concentration of 0–500 µmol L$^{-1}$. b) Short-circuit current of liquid–solid TENG in oil/water (pH 8.5 Tris-HCl buffer) multiphase after being modified by dopamine with concentration of 0–500 µmol L$^{-1}$. c,d) Plots of oil/water interfacial current ($I_{interface}$) and $I_{TENG}$ versus concentration of dopamine from 0 to 500 µmol L$^{-1}$. Inset of (c,d): Plots of $I_{interface}$ and $I_{TENG}$ as a function of ln($C$), where $C$ is the concentration of dopamine.

and accordingly, the interfacial signal appears from the second cycle and gradually increases until a stable output is reached.

To investigate the linear relationship between the dual signals and dopamine concentration, the TENG was reacted with different concentrations of dopamine from 0 to 500 µmol L$^{-1}$, and then the short-circuit current was measured at an operating speed of 0.05 m s$^{-1}$. **Figure 4**a shows the contact angle of water on the TENG surface after reacting with different concentrations of dopamine. The contact angle decreases with increasing dopamine concentration, indicating that the hydrophilicity of the TENG surface increases with increasing dopamine concentration, which can be attributed to the increased amount of adsorbed PDA on the TENG surface through self-polymerization of dopamine. The dependence between short-circuit current and dopamine concentration is shown in Figure 4b–d. The $I_{interface}$ gradually increased with increasing dopamine concentration from 0 to 500 µmol L$^{-1}$ (Figure 4c). A good linear relationship between the value of $I_{interface}$ and natural logarithm of dopamine concentration over the range from 25 to 500 µmol L$^{-1}$ is shown in the inset of Figure 4c. The fitted trend line can be expressed as $I_{interface} = 4.40 + 1.11 \times \ln C_{(Dopamine)}$ ($R^2 = 0.99$). In contrast to the $I_{interface}$, the $I_{TENG}$ gradually decreases as the dopamine concentration increases (Figure 4d). The inset of Figure 4d shows the good linear relationship between the value of $I_{TENG}$ and natural logarithm of dopamine concentration over the range from 25 to 250 µmol L$^{-1}$, which is consistent with the results of short-circuit current of TENG in a single water multiphase (Figure S11, Supporting Information). The fitted

trend line can be expressed as $I_{TENG} = 22.78 - 3.96 \times \ln C_{(Dopamine)}$ ($R^2 = 0.98$). The limit of detection (LOD) of dopamine for $I_{interface}$ and $I_{TENG}$ is calculated to be 3.96 and 5.15 µM, respectively, from the formula of $3S_b/k$, where $S_b$ is the standard deviation of the blank and $k$ was the slope of the fitted trend line. These results demonstrate the good potential of the dual signals, which are generated simultaneously by the liquid–solid TENG in oil/water multiphase, as a sensitive biochemical sensing platform.

In summary, we reported a liquid–solid contact TENG for harvesting energy in oil/water multiphase. There are two distinctive signals being generated when the liquid–solid contact TENG is insert into the oil/water multiphase; one is from the contact electrification and electrostatic induction between the liquid and the PTFE film, and the other one is from the electrostatic induction in the copper electrode by the oil/water interfacial charges. These two featured signals have been successfully demonstrated for self-powered dual-signal sensing of dopamine. The two signals show interesting opposite changing trends that the $V_{TENG}$ and $I_{TENG}$ decrease while the oil/water interfacial signals of $\Delta V_{interface}$ and $I_{interface}$ increase after functioning a layer of PDA on the surfaces of PTFE and glass via self-polymerization. Both the value of $I_{TENG}$ and $I_{interface}$ have a good linear relationship versus natural logarithm of concentration of dopamine. To the best of our knowledge, this is the first self-powered dual-signal biochemical sensing platform based on TENG. We believe that this concept will contribute to more reliable and advanced self-powered dual-signal sensors.

## Experimental Section

*Fabrication of TENG*: A plain glass slide (75 mm × 25 mm × 1 mm) was used as substrate. The glass slide was washed with a detergent followed by ultrasonicating 30 min in ethanol. After drying in a 60 °C oven, a layer of copper electrode was deposited on the surface of the glass slide substrate by PVD method. Then, an electrification thin film made of PTFE was tightly adhered to the surface of the glass slide on the copper electrode side to insulate the copper electrode from the surrounding liquid. The surface of the TENG was then cleaned with ethanol and dried with $N_2$ gas.

*Surface Modification with PDA Layer*: A series of dopamine solutions with different concentrations are prepared in Tris–HCl buffer (pH 8.5). The TENG was rinsed with ethanol before coating and then immersed in a dopamine solution, followed by stirring for 12 h. The coated TENGs were rinsed with water and dried with $N_2$ gas for subsequent electrical output measurements.

*Electrical Output Measurements*: The open-circuit voltage and short-circuit current of the TENG device were measured by a Keithley 6514 system electrometer. The TENG was operated using a linear motor by periodically inserting it into and pulling out of solution to generate electric output. 50 mL aqueous phase solution and 20 mL oil were sequentially added to a glass beaker to form a multiphase system for the electrical output measurements in oil/water multiphase.

## Supporting Information

Supporting Information is available from the Wiley Online Library or from the author.

## Acknowledgements

## Conflict of Interest

The authors declare no conflict of interest.

## Keywords

[1] a) F. R. Fan, Z. Q. Tian, Z. L. Wang, *Nano Energy* **2012**, *1*, 328; b) Z. L. Wang, *ACS Nano* **2013**, *7*, 9533; c) Z. L. Wang, J. Chen, L. Lin, *Energy Environ. Sci.* **2015**, *8*, 2250.

[2] a) Y. Jie, N. Wang, X. Cao, Y. Xu, T. Li, X. Zhang, Z. L. Wang, *ACS Nano* **2015**, *9*, 8376; b) Z. H. Lin, G. Zhu, Y. S. Zhou, Y. Yang, P. Bai, J. Chen, Z. L. Wang, *Angew. Chem., Int. Ed.* **2013**, *52*, 5065; c) Z. Li, J. Chen, J. Yang, Y. Su, X. Fan, Y. Wu, C. Yu, Z. L. Wang, *Energy Environ. Sci.* **2015**, *8*, 887; d) Y. K. Jung, K. N. Kim, J. M. Baik, B. S. Kim, *Nano Energy* **2016**, *30*, 77; e) Z. H. Lin, Y. Xie, Y. Yang, S. Wang, G. Zhu, Z. L. Wang, *ACS Nano* **2013**, *7*, 4554.

[3] V. Nguyen, R. Yang, *Nano Energy* **2013**, *2*, 604.

[4] a) G. Zhu, Y. Su, P. Bai, J. Chen, Q. Jing, W. Yang, Z. L. Wang, *ACS Nano* **2014**, *8*, 6031; b) Z. H. Lin, G. Cheng, L. Lin, S. Lee, Z. L. Wang, *Angew. Chem., Int. Ed.* **2013**, *52*, 12545; c) L. Pan, J. Wang, P. Wang, R. Gao, Y. C. Wang, X. Zhang, J. J. Zou, Z. L. Wang, *Nano Res.* **2018**, *11*, 4062; d) J. Wang, Z. Wu, L. Pan, R. Gao, B. Zhang, L. Yang, H. Guo, R. Liao, Z. L. Wang, *ACS Nano* **2019**, *13*, 2587.

[5] a) J. Nie, Z. Ren, J. Shao, C. Deng, L. Xu, X. Chen, M. Li, Z. L. Wang, *ACS Nano* **2018**, *12*, 1491; b) X. Li, M. H. Yeh, Z. H. Lin, H. Guo, P. K. Yang, J. Wang, S. Wang, R. Yu, T. Zhang, Z. L. Wang, *ACS Nano* **2015**, *9*, 11056; c) J. Chen, H. Guo, J. Zheng, Y. Huang, G. Liu, C. Hu, Z. L. Wang, *ACS Nano* **2016**, *10*, 8104; d) S. B. Jeon, M. L. Seol, D. Kim, S. J. Park, Y. K. Choi, *Adv. Electron. Mater.* **2016**, *2*, 1600006; e) K. Liu, T. Ding, X. Mo, Q. Chen, P. Yang, J. Li, W. Xie, Y. Zhou, J. Zhou, *Nano Energy* **2016**, *30*, 684; f) B. D. Chen, W. Tang, C. He, T. Jiang, L. Xu, L. P. Zhu, G. Q. Gu, J. Chen, J. J. Shao, J. J. Luo, Z. L. Wang, *Adv. Mater. Technol.* **2018**, *3*, 1700229.

[6] M. E. Leunissen, A. van Blaaderen, A. D. Hollingsworth, M. T. Sullivan, P. M. Chaikin, *Proc. Natl. Acad. Sci. USA* **2007**, *104*, 2585.

[7] J. C. Carruthers, *Trans. Faraday Soc.* **1938**, *34*, 300.

[8] W. Dickinson, *Trans. Faraday Soc.* **1941**, *37*, 140.

[9] J. K. Beattie, A. M. Djerdjev, *Angew. Chem., Int. Ed.* **2004**, *43*, 3568.

[10] H. Zou, Y. Zhang, L. Guo, P. Wang, X. He, G. Dai, H. Zheng, C. Chen, A. C. Wang, C. Xu, Z. L. Wang, *Nat. Commun.* **2019**, *10*, 1427.

[11] X. J. Zhao, G. Zhu, Y. J. Fan, H. Y. Li, Z. L. Wang, *ACS Nano* **2015**, *9*, 7671.

[12] a) K. Yatsuzuka, Y. Mizuno, K. Asano, *J. Electrost.* **1994**, *32*, 157; b) B. Ravelo, F. Duval, S. Kane, B. Nsom, *J. Electrost.* **2011**, *69*, 473.

[13] J. K. Beattie, A. M. Djerdjev, G. G. Warr, *Faraday Discuss.* **2009**, *141*, 31.

[14] K. G. Marinova, R. G. Alargova, N. D. Denkov, O. D. Velev, D. N. Petsev, I. B. Ivanov, R. P. Borwankar, *Langmuir* **1996**, *12*, 2045.

[15] P. Creux, J. Lachaise, A. Graciaa, J. K. Beattie, A. M. Djerdjev, *J. Phys. Chem. B* **2009**, *113*, 14146.

[16] P. Creux, J. Lachaise, A. Graciaa, J. K. Beattie, *J. Phys. Chem. C* **2007**, *111*, 3753.

[17] a) Y. Lan, F. Yuan, T. H. Fereja, C. Wang, B. Lou, J. Li, G. Xu, *Anal. Chem.* **2019**, *91*, 2135; b) Q. Yuan, Y. Liu, C. Ye, H. Sun, D. Dai, Q. Wei, G. Lai, T. Wu, A. Yu, L. Fu, K. W. A. Chee, C. T. Lin, *Biosens. Bioelectron.* **2018**, *111*, 117.

[18] Y. Fang, S. Gonuguntla, S. Soh, *ACS Appl. Mater. Interfaces* **2017**, *9*, 32220.